01 Jan 2007

Evidence of Dynamical Spin Shielding in Ce from Spin-Resolved Photoelectron Spectroscopy

James G. Tobin

S. W. Yu

Takashi Komesu

B. W. Chung

et. al. For a complete list of authors, see https://scholarsmine.mst.edu/phys_facwork/58

Recommended Citation

J. G. Tobin et al., "Evidence of Dynamical Spin Shielding in Ce from Spin-Resolved Photoelectron Spectroscopy," *Europhysics Letters*, Institute of Physics - IOP Publishing, Jan 2007.
The definitive version is available at https://doi.org/10.1209/0295-5075/77/17004

A Letters Journal Exploring the Frontiers of Physics

January 2007

EPL, **77** (2007) 17004
doi: 10.1209/0295-5075/77/17004

www.epljournal.org

Evidence of dynamical spin shielding in Ce from spin-resolved photoelectron spectroscopy

J. G. Tobin[1(a)], S. W. Yu[1], T. Komesu[2], B. W. Chung[1], S. A. Morton[1,2(b)] and G. D. Waddill[2]

[1] *Lawrence Livermore National Laboratory - Livermore, CA, USA*
[2] *University of Missouri-Rolla - Rolla, MO, USA*

received 29 July 2006; accepted in final form 7 November 2006
published online 5 January 2007

PACS 71.28.+d – Narrow-band systems; intermediate-valence solids
PACS 72.25.Fe – Optical creation of spin polarized carriers
PACS 79.60.-i – Photoemission and photoelectron spectra

Abstract – Using Fano effect measurements upon polycrystalline Ce, we have observed a phase reversal between the spectral structure at the Fermi edge and the other $4f$ derived feature near a binding energy of 2 eV. The Fano effect is the observation of spin polarized photoelectron emission from *nonmagnetic* materials, under chirally selective excitation, such as circularly polarized photons. The observation of phase reversal between the two peaks is a direct experimental proof of Kondo shielding in Ce, confirming the predictions of Gunnarsson and Shoenhammer, albeit with a small modification.

Electron correlation is perhaps the last, great unknown in the study of the electronic structure of materials. The conventional experimental approach to the problem is to test the various predictions of different models by interrogating complex systems with photoelectron spectroscopy of very high energy and angular momentum [1–3]. Here, we report of a study performed in a different mode, wherein the central issue of most electron correlation models can be directly addressed, *i.e.* shielding of unpaired spins. By performing photoelectron spectroscopy with a different type of high resolution, using chiral excitation and true spin resolution [4,5], it has been possible to probe directly the phase relationships of the valence band features in Ce. Below, it will be shown that the shielding of the unpaired spin (in the lower Hubbard band, LHB, or f^0 peak) by the electrons in the quasiparticle peak (f^1 or Kondo peak, near the Fermi energy) has been observed in the case of polycrystalline Ce. (See fig. 1.)

For many years, the valence electronic structure and corresponding electron spectra of cerium have remained subjects of uncertainty and controversy. (For a fuller description of this issue, please see ref. [5] and the references therein.) Much of the controversy revolves around the interpretation of the Ce photoemission structure in terms of a modified Anderson impurity model [6–8]. In this correlated and multi-electronic picture, proposed by Gunnarsson and Schoenhammer [6,7], semi-isolated $4f$ states (at a nominal binding energy of 1 eV) are in contact with the bath of *spd* valence electrons, generating spectral features at the Fermi level and at a binding energy corresponding to the depth of the bath electron well, about 2 eV below the Fermi level in the case of Ce. The picture is a specific case of a more generalized model in which the crucial element is the competition between the bandwidth (W) and correlation strength (U), as discussed by Kotliar and Vollhardt [9]. We have applied circularly polarized soft X-rays and true spin detection, in a modified form of the photoelectron spectroscopy experiment, to the enigmatic Ce system. The result of this is that we have observed the first experimental proof of Kondo shielding, the central tenet of the Gunnarsson-Schoenhammer picture, using Fano effect measurements [10,11]. (The Fano effect is the observation of spin specific photoelectron emission from the valence bands of a nonmagnetic material due to excitation with circularly polarized light. A more complete description of this issue and appropriate references can be found in ref [5].)

The experiments were performed at the Advanced Light Source (ALS) at Lawrence Berkeley National Laboratory, the Advanced Photon Source (APS) at Argonne National Laboratory and Lawrence Livermore National Laboratory. Ultra-pure Ce samples were grown *in situ* under UHV conditions, by evaporation onto W substrates at

(a) E-mail: Tobin1@LLNL.Gov
(b) Present address: Advanced Light Source, Lawrence Berkeley National Laboratory - Berkeley, CA, USA.

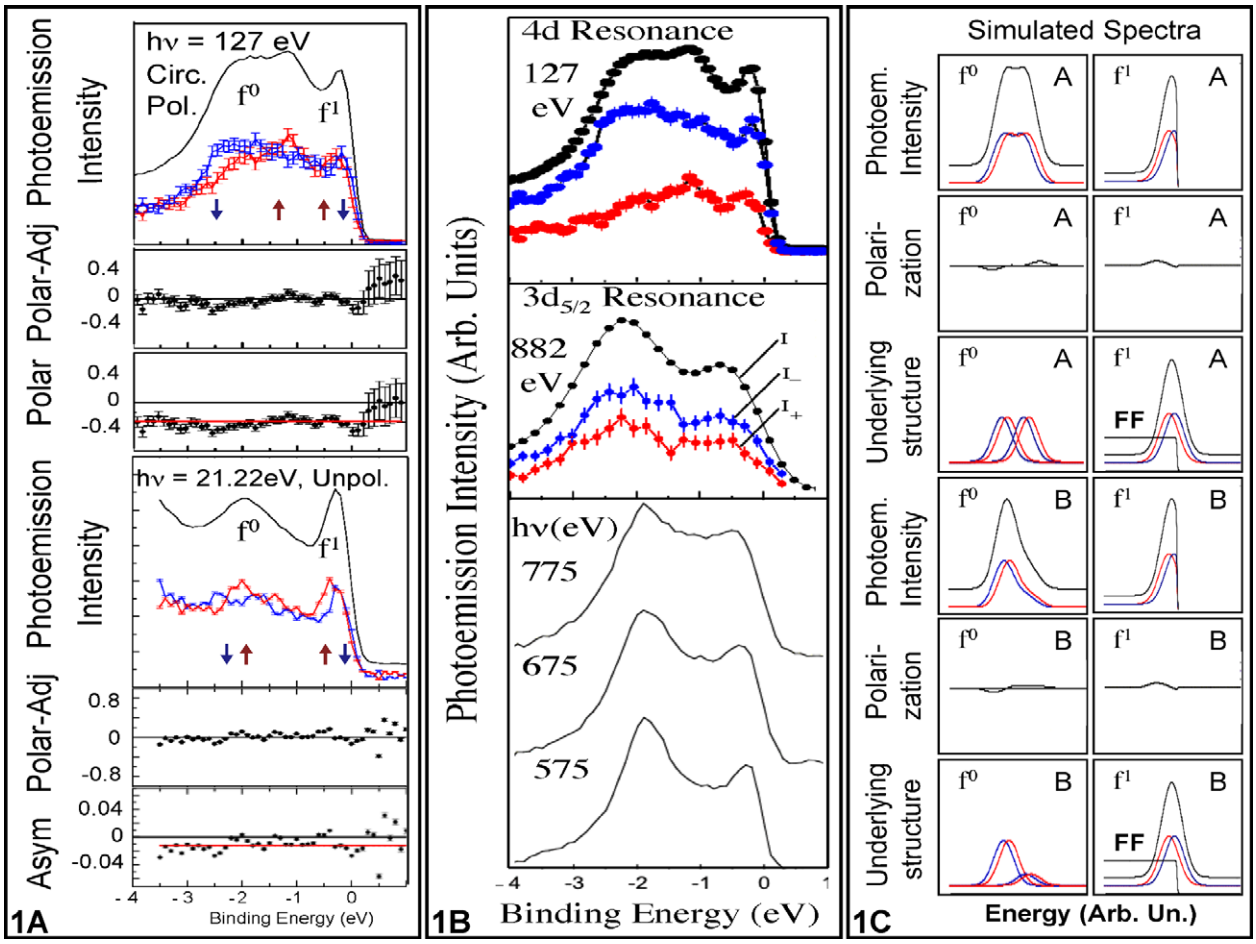

Fig. 1: A) Spin-resolved (blue and red) and spin-integrated spectra (black) of polycrystalline Ce are shown here, along with corresponding polarizations and asymmetry data [4,5]. Error bars for the spin-resolved spectra are included. Blue (red) corresponds to spin-down (up). See text for details. B) Top panel: spin-resolved and spin-integrated spectra of polycrystalline Ce at the $4d$ to $4f$ resonance. Middle panel: spin-resolved and spin-integrated spectra of polycrystalline Ce at the $3d_{5/2}$ resonance. Bottom panel: spin-integrated spectra of polycrystalline Ce. Color conventions follow those of A). The energy bandwidth was 0.32 eV at 575 eV, 0.43 eV at 675 eV and 0.56 eV at 775 eV. Thus the resolving power ($E/\Delta E$) in each case was near 1500. C) Spectral simulations for cases A and B, as described in the text. Color conventions follow those of A) and fig. 2. FF stands for Fermi function.

room temperature. This process gives rise to what is nominally referred to as polycrystalline γ-Ce, with all of the attendant issues of multiple phase contributions and surface *vs.* bulk effects [4,5]. Details of the instruments, experimental setups and data analysis are described elsewhere [4,5]. However, the general principle of the experiment can be summarized as follows. By using a chiral probe, such as circularly polarized X-rays, for the excitation in conjunction with true spin detection, one is able to obtain a spin-sensitivity in *nonmagnetic* systems. The circularly polarized radiation establishes an axis of quantization that can be inverted by reversing the helicity of the circularly polarized radiation. In the same way that spectra in ferro-magnetic systems are collected for both directions of macroscopic magnetization, data in the nonmagnetic systems are collected for both circular polarizations, thus allowing for the determination and removal of instrumental asymmetries. Because of the short-time structure for the X-ray absorption and photoemission event (10^{-15} s–10^{-18} s), this measurement is potentially fast enough to probe the dynamic shielding hypothesized for electron correlated systems. Finally, the success of this method is predicated upon the presence of a spin-orbit splitting and the predominance of localized effects in the electronic structure. Strong itinerancy would wash out the effects being sought by this measurement. Thus, observations of strong Fano dichroic effects have been made in the past for core levels in nonmagnetic systems, with both circular and linear polarization (fig. 2A and refs. [5,12–14]). The issue for Ce was simple: could this work for the valence states?

As can be seen in fig. 1A, we have indeed observed Fano dichroic effects in the valence states of Ce polycrystalline films. In the top panel, data on the $4d$ to $4f$ resonance is shown. The advantage of being on resonance is the improvement of the counting rates owing to the

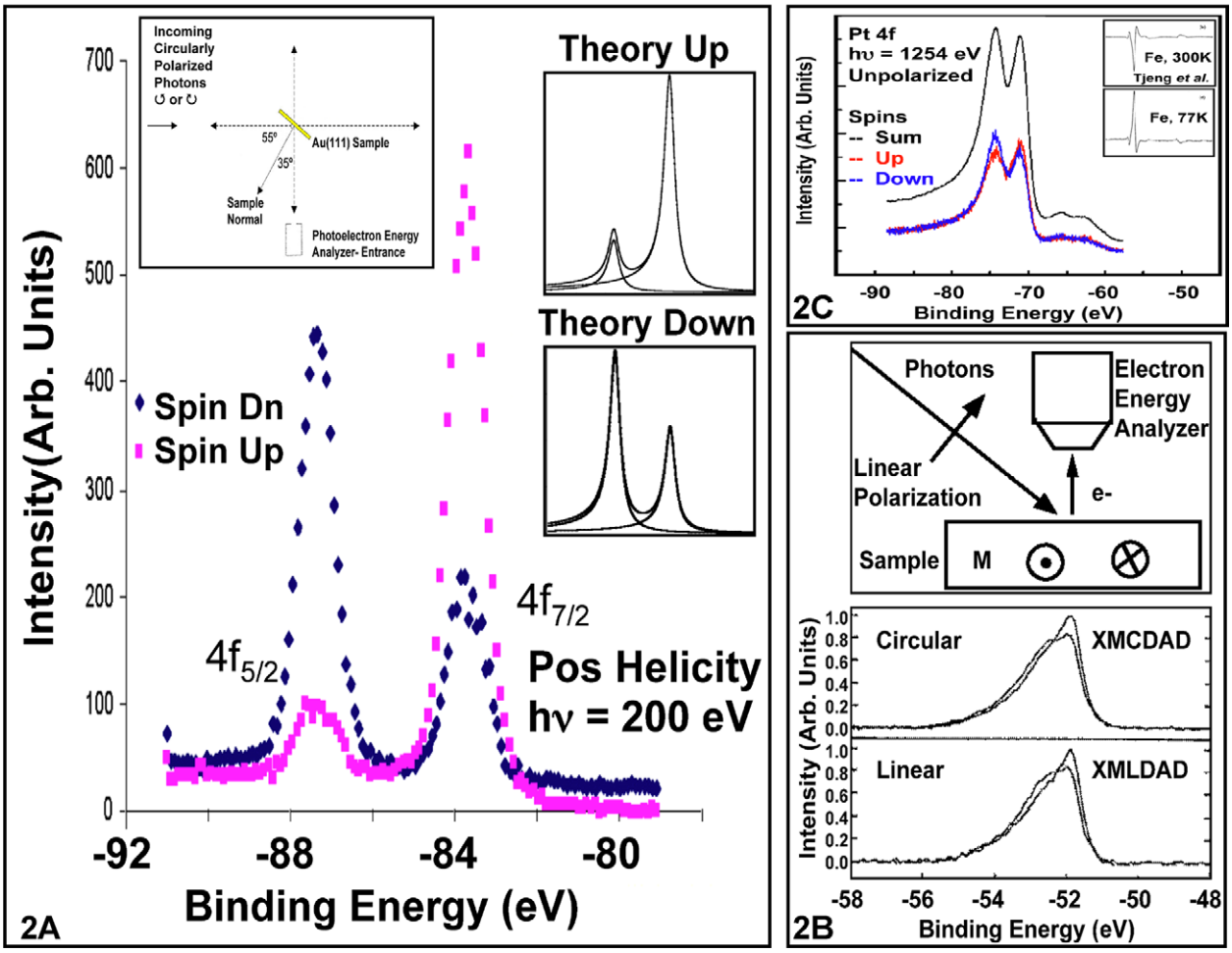

Fig. 2: A) Fano effect results for Au $4f$ core states with circular polarization and true spin detection. The experimental spin-resolved results are shown in color. The experimental geometry diagram is in the inset in the upper left and the results of a simple theory are in the insets in the upper right. See text for details. B) In the lower panel, the results of a photoelectron dichroic experiment upon $Fe_{50\%}Ni_{50\%}/Cu(001)$ is shown here. XML(C)DAD is X-ray magnetic linear (circular) dichroism in angular distributions. The photon energy was 95 eV. The experimental geometry for the XMLDAD experiment is shown in the top panel. M is the sample magnetization, into and out of the plane of the figure. See the text for details. C) The measurements of the Fano effect of the Pt $4f$ states, using unpolarized MgK-alpha radiation is shown here. Please see the text for details. The phase reversal of the Fe $2p$ dichroism, from Tjeng *et al.* [20] is shown in the inset in the upper right. When the Gd in the garnet orders magnetically, the antiferromagnetically coupled Fe's reverse their phase.

larger cross-sections. The disadvantage is the somewhat increased complexity owing to the presence of the indirect channel of resonant photoemission along with the usual direct channel of regular photoemission. In this case, the additional complexity manifests itself in two ways: 1) a large static polarization associated with the the dominance of singlet coupling in the indirect channel decay path (figs. 1A, B and ref. [4]) and 2) the presence of an additional strong sub-feature at a binding energy of 1 eV [15,16]. The solution for the first problem is simple: by subtracting off a constant polarization from the "raw" polarization shown in the third panel from the top in fig. 1A, an adjusted polarization is obtained (shown in the second panel of fig. 1A) and from the adjusted polarization and the integrated spectrum, it is then possible to generate the spin-resolved spectra shown in the top panel of fig. 1A. Here it is clear that there is an underlying spin structure in the valence states of Ce. The second issue, the presence of the fairly strong sub-feature at 1 eV binding energy will be addressed in more detail below.

Furthermore, it is possible to observe similar effects in an off resonance experiment. In the lower half of fig. 1A, results are shown for data collected in a chiral configuration, using unpolarized HeI radiation at an energy of 21.22 eV. Although conceptually more convolved than the case using circular polarization, the data collected in this mode is essentially equivalent with that collected using circularly polarized X-rays, as will be described next.

First, it has been established that under many conditions X-ray magnetic linear dichroism in photoelectron spectroscopy provides essentially the same information as provided by X-ray magnetic circular dichroism in

photoelectron spectroscopy [17,18]. An example of this is shown in fig. 2B. Here a dichroic photoemission experiment upon a ferromagnetic sample is done in two different ways, giving rise to essentially identical results [17]. The samples were $Fe_{50\%}Ni_{50\%}/Cu(001)$. One data set was collected using circular polarization, in a configuration similar to that diagrammed in fig. 2A. The other data set was collected using a chiral configuration of linear vectors, as illustrated in fig. 2B. Here, almost all of the important linear vectors (the direction of propagation and polarization of the photons, the emission direction of the collected electrons, and some of the crystallographic axes of the sample) are in the horizontal plane. Only the magnetization vector (M) breaks the symmetry. As can be seen in fig. 2B, the XMCDAD and XMLDAD from magnetization reversal are essentially identical. Theoretically, they are each dependent upon the imaginary and real parts of the same matrix elements, respectively. In this case, symmetry reversal is achieved by inverting the magnetic field. Reversing the XMLDAD configuration would require a new experimental geometry, that would be the mirror image of the configuration shown in fig. 2B.

Second, because of the vectorially chiral selection rules for these processes, unpolarized radiation can produce the same effect, albeit with about twice the background (and thus about 1/2 of the percentage dichroism) relative to properly linearized polarization [19]. An example of this is shown in fig. 2C. Here, a configuration of vectors, similar to that in fig. 2B, is utilized. However, in this case, the electromagnetic radiation (photons) is completely unpolarized and spin is substituted for the magnetization (M) as the symmetry breaking vector, analogous to to the experiment in fig. 2A. In terms of cross-sectional dependences, it is possible to divide the contributions into a set derived from the in-plane component (as in fig. 2B) and a set derived from the out-of-plane component. The in-plane component can generate a dichroic response but the out-of-plane component will not. The out-of-plane component can contribute to the overall intensity, but not the dichroism. The relative magnitude of the dichroism is reduced, as is evident from a comparison of figs. 2A and C. Thus, here is the observation of a Fano effect in a core level of a nonmagnetic material, with unpolarized photons and true spin detection, driven by the vectorial chirality of the experimental vectors.

Now, return to a consideration of Ce and fig. 1. Unfortunately, because the chirality of this experiment is induced by the orientation of the Poynting vector of the incoming X-rays and the emission direction of the electrons relative to the perpendicularly aligned spin, chirality reversal is very difficult and requires a physical reconfiguration of the experimental apparatus. Thus, we chose to instead perform the experiment in one configuration and remove the instrumental asymmetry mathematically. The static offset in the asymmetry (shown in the bottommost panel of fig. 1A) has been subtracted from the "raw" polarization, to provide an adjusted polarization, shown in the second panel from the bottom. From this adjusted polarization and the integrated photoemission spectra, the spin-resolved spectra in the third panel from the bottom have been generated. (Alternate forms of asymmetry removal were also pursued, each producing essentially the same result shown in fig. 1A.) Again a significant spin polarization of the Ce valence bands is observed, similar to but not quite identical with that of the data in the topmost panel of fig. 1A.

Additional information regarding the nature of these states can be gleaned from spin-integrated photoelectron spectroscopy. The data in fig. 1B demonstrates the strong f-character and bulk nature of both features. In the Ce $4f$ resonant photoemission, the increase in cross-section is driven by the addition of an auxiliary channel involving either a $3d$ or $4d$ core level. Because of the strong dipole selection rules, the amplification is f-state specific. Thus, the observation of enhancement of both the Fermi level feature and the higher binding energy feature in the $4d$ resonance and the $3d$ resonance indicates that both states have a strong and roughly equivalent degree of f-character. In the bottommost panel of fig. 1B, a series of spectra at higher photon energies but below the $3d$ threshold are shown. Except for smearing of the features due to increasing energy bandwidth as the photon energy increases, the relative magnitudes of the two features remain fairly constant and consistent with that of the spin-integrated spectra in fig. 1A. Following the lead of Mo *et al.* [3], this leads to the conclusion that both features are bulk derived. The importance of these two observations will become clear in the discussion, which follows below.

From the utilization of simple spectral simulations, it is possible to gain significant insight into the nature of what is driving these observed spin polarizations. The success of these spectral simulations is illustrated in fig. 2A. Here, a simple model based upon electric dipole transitions with circularly polarized excitation can simulate the observed experimental results for the Au $4f$ states. This model includes the proper treatment of state specific transitions, intensities and Doniach-Sunjic lineshapes, analogous to that derived earlier for the Fe $3p$ case [17].

Now consider the situation for the Ce $4f$ states, as shown in fig. 1C. Here we have a fairly broad individual peak width with only a small spin-orbit splitting. In case A, corresponding to the resonant PES data at $h\nu = 127\,\mathrm{eV}$, three sets of spin orbit split peaks are used. The pair near the Fermi energy, with spin-down leading spin-up, is truncated by the Fermi function. The effect of this is to produce two peaks with essentially the same Fermi edge but different widths. The other two peaks, corresponding to the symmetric and anti-symmetric states observed by Vyalikh *et al.* [15], each have spin-up leading spin-down. This closely-spaced pair of sub-features combines to produce a broadened integrated peak and spin structure, with polarity reversed relative to the Fermi energy peak. In case B, corresponding to the off-resonance PES data at $h\nu = 21.22\,\mathrm{eV}$, three sets of

peaks are again used, but this time one of them is reduced in intensity relative to the other two. The same structure is observed near the Fermi energy as in case A, but the higher binding energy feature is now more skewed and exhibits a more narrowly spaced polarization. Nevertheless, this polarization retains the reversed phase relative to the Fermi level peak. Thus, the central observation here is that there is a phase reversal between the spectral feature at the Fermi level and that at higher binding energies.

The phase reversal, coupled with the previously demonstrated bulk-nature and f-character of both features, is a direct proof of dynamical spin shielding in Ce. Phase reversals in dichroic studies have been observed before [20,21] and an example is reproduced in fig. 4 from Tjeng *et al.* [20], where anti-ferromagnetic coupling in a garnet reverses the dichroism in the Fe $2p$ states. However, in these previous studies some sort of net magnetization was present and the direction of the phase can be affected by the site symmetry and the orbital momentum parentage of the states. In the case of Ce, the situation is different. The similar parentage of both features, with a strong f-character contribution, means that there should be no phase reversal unless there is a spin counter-alignment. Moreover, these Fano effect measurements are dynamic. There is *no* net magnetic vector in Ce. Thus the spin counter-alignment is exactly that hypothesized by Gunnarsson and Schoenhammer in 1983 [6,7]. However, there is one inconsistency relative to the picture of Gunnarsson and Schoenhammer, which assigned the 2 eV peak (f^0 or LHB) as being f derived and the peak at the Fermi energy (f^1 or Kondo) as being of valence band (*spd*) character. Nevertheless, a recent work by Georges [22] suggests that the same species can screen itself, in something like a Hubbard picture with only one type of electron species, within a dynamical mean-field theory (DMFT) computational scheme. In his DMFT modeling of a Mott transition, he finds that "Electrons are itinerant in the metallic phase, and the moments are quenched. Within DMFT this quenching is akin to a (self-consistent) local Kondo effect." It may not be unreasonable to expect that a DMFT extension of the GS model would ultimately mix the states to the degree that they would seem to be of the same species, with both possessing significant f-character.

In summary, it has been demonstrated that 1) both spectral features in the valence bands of Ce are bulk derived and possessing significant f-character and 2) there is a dynamic spin counter alignment between the two features. These facts, taken together, confirm the original picture of Gunnarsson and Shoenhammer, with the minor modification of state mixing between the two features. This study also illustrates the efficacy and potential of using the Fano effect to probe spin correlation in nonmagnetic systems. Our future plans include the extension of these measurements to single crystals of Ce and Ce alloys, to more properly address the predicted phase specific properties of Ce [23–27].

* * *

This work was performed under the auspices of the US DOE by University of California Lawrence Livermore National Laboratory under contract W-7405-Eng-48. The ALS and APS have been built and operated under funding from the Office of Basic Energy Science at DOE. Conversations with A. McMahan were highly enlightening and greatly appreciated. Work by LLNL and UMR personnel was supported by OBES/DOE.

REFERENCES

[1] Shen K. M., Ronning F., Lu D. H., Baumberger F., Ingle N. J. C., Lee W. S., Meevasana W., Kohsaka Y., Azuma M., Takano M., Takagi H. and Shen Z.-X., *Science*, **307** (2005) 901 and references therein.

[2] Souma S., Machida Y., Sato T., Takahashi T., Matsui H., Wang S.-C., Ding H., Kaminski A., Campuzano J. C., Sasaki S. and Kadowaki K., *Nature*, **423** (2003) 65 and references therein.

[3] Mo S.-K., Denlinger J. D., Kim H.-D., Park J.-H., Allen J. W., Sekiyama A., Yamasaki A., Kadono K., Suga S., Saitoh Y., Muro T., Metcalf P., Keller G., Held K., Eyert V., Anisimov V. I. and Vollhardt D., *Phys. Rev. Lett.*, **90** (2003) 186403 and references therein.

[4] Yu S. W., Komesu T., Chung B. W., Waddill G. D., Morton S. A. and Tobin J. G., *Phys. Rev. B*, **73** (2006) 075116 and references therein.

[5] Tobin J. G., Morton S. A., Chung B. W., Yu S. W. and Waddill G. D., *Physica B*, **378-380** (2006) 925 and references therein.

[6] Gunnarsson O. and Schoenhammer K., *Phys. Rev. Lett*, **50** (1983) 604.

[7] Gunnarsson O. and Schoenhammer K., *Phys. Rev. B*, **28** (1983) 4315.

[8] Allen J. W. and Liu J. Z., *Phys. Rev. B*, **46** (1992) 5047.

[9] Kotliar G. and Vollhardt D., *Phys. Today*, **57** (2004) 53 and references therein.

[10] Fano U., *Phys. Rev.*, **178** (1969) 131; **184** (1969) 250.

[11] Heinzmann U., Kessler J. and Lorenz J., *Phys. Rev. Lett.*, **25** (1970) 1325.

[12] Starke K., Kaduwela A. P., Liu Y., Johnson P. D., Van Hove M. A., Fadley C. S., Chakarian V., Chaban E. E., Meigs G. and Chen C. T., *Phys. Rev. B*, **53** (1996) R10544.

[13] Roth C., Hillebrecht F. U., Park W. G., Rose H. B. and Kisker E., *Phys. Rev. Lett.*, **73** (1994) 1963.

[14] Rose H. B., Fanelsa A., Kinoshita T., Roth C., Hillebrecht F. U. and Kisker E., *Phys. Rev. B*, **53** (1996) 1630.

[15] Vyalikh D. V., Kucherenko Yu., Danzenbächer S., Dedkov Yu. S., Laubschat C. and Molodtsov S. L., *Phys. Rev. Lett.*, **96** (2006) 026404.

[16] Jensen E. and Weiliczka D. M., *Phys. Rev. B*, **30** (1984) 7340.

[17] Tobin J. G. and Schumann F. O., *Surf. Sci.*, **478** (2001) 211 and references therein.
[18] Venus D., *Phys. Rev. B*, **48** (1993) 6144; **49** (1994) 8821.
[19] Schneider C. M., Pracht U., Kuch W., Chassé A. and Kirschner J., *Phys. Rev. B*, **54** (1996) R15618.
[20] Tjeng L. H., Rudolf P., Meigs G., Sette F., Chen C. T. and Idzerda Y. U., *Proc. SPIE*, **1548** (1991) 160.
[21] Holm A. P., Kauzlarich S. M., Morton S. A., Waddill G. D., Pickett W. E. and Tobin J. G., *J. Am. Chem. Soc.*, **124** (2002) 9894.
[22] Antoine Georges, arXuv:cond-mat/0403123 v1 (2004/ 2005), see fig. 17, p. 48.
[23] Held K., McMahan A. K. and Scarlettar R. T., *Phys. Rev. Lett.*, **87** (2001) 276404; McMahan A. K., Held K. and Scarlettar R. T., *Phys. Rev. B*, **67** (2003) 075108.
[24] Zölfl M. B., Nekrasov I. A., Pruschke Th., Anisimov V. I. and Keller J., *Phys. Rev. Lett.*, **87** (2001) 276403.
[25] Haule K., Oudovenko V., Savrasov S. Y. and Kotliar G., *Phys. Rev. Lett.*, **94** (2005) 036401.
[26] de' Medici L., Georges A., Kotliar G. and Biermann S., *Phys. Rev. Lett.*, **95** (2005) 066402.
[27] Amadon B., Biermann S., Georges A. and Aryasetiawan F., *Phys. Rev. Lett.*, **96** (2006) 066402.